Numerical study for unsteady Casson fluid flow with heat flux using a spectral collocation method

M. M. Khader[1,2]

[1]Department of Mathematics and Statistics, College of Science, Imam Mohammad Ibn Saud Islamic University (IMSIU), Riyadh, Saudi Arabia

[2]Department of Mathematics, Faculty of Science, Benha University, Benha, Egypt

Email: mohamed.khader@fsc.bu.edu.eg

Abstract

An efficient numerical method is presented in this study to discuss the effects of variable heat flux, viscous dissipation and the slip velocity on the viscous Casson flow and heat transfer due to an unsteady stretching sheet taking into account the influence of heat generation or absorption. Industrially, this type of fluid can describe the flow of blood in an industrial artery, which can be polished by a material governing the blood flow. The spectral collocation method based on Chebyshev polynomials of the third-kind is employed to solve the resulting system of ordinary differential equations which describe the problem. Influence of the parameters governing the flow and heat transfer such as unsteadiness parameter, slip velocity parameter, Casson parameter, local Eckert number, heat generation parameter and the Prandtl number are discussed and presented through tables and graphs. Also, the local skin-friction coefficient and the local Nusselt number at the stretching sheet are computed and discussed. Finally, the results show that the given procedure is an easy and efficient tool to investigate the solution of such fluid models.

Keywords: Non-Newtonian Casson flow; Unsteady stretching sheet; Variable heat flux; Slip effect; Viscous dissipation; Heat generation; Chebyshev-spectral collocation method.

MSC 2010: 41A30; 65N12; 65M60; 76F12.

1. Introduction

Flow and heat transfer due to an unsteady stretching sheet has attracted an ever increasing research interest because of it's numerous practical applications in many branches of manufacturing processes and technology since Crane [1] presented analytically the solution for the problem of steady flow for a Newtonian fluid driven by a stretched flat sheet which moves in its own plane with a velocity varying linearly with the distance from a fixed point. The problem posed by Crane [1] was extended taking into account a porous sheet by Gupta and Gupta [2] and they also, obtained closed-form solution for the problem, while Grubka and Bobba [3] investigated the thermal field and they introduced the solution for the energy equation in terms of Kummers functions. In the same field of study, many researches are also introduced [4]-[12].

In nature, several fluids can be classified as Casson fluid. This type of fluids can be marked as a purely viscous fluid with high viscosity. Some of studies related to this type of fluid may be found in [13]-[15]. Most of previous studies have neglected the slip velocity condition at the boundary over a stretching surface which is important in view point of desired properties of the outcome. The fluids that exhibit boundary slip have important technological applications such as in the polishing of artificial heart valves and internal cavities. Because of important various applications for the flow and heat transfer characteristics in the presence of slip effects over a stretching surface, a lot of papers were found [16]-[19].

After these former researches, a number of researchers have successfully applied various numerical methods in this field. Among these numerical methods, the spectral collocation method (SCM) that is a general approximate analytical method to get the approximate solution of the differential equations. The SCM has some advantages for handling this class of problems in which the Chebyshev coefficients for the solution can exist very easily after using any one of numerical programs. For this reason, this method is much faster than the other methods. Chebyshev polynomials are well-known family of orthogonal polynomials on the interval $[-1, 1]$ that have many applications. They are widely used because of their good properties in the approximation of functions. Also, this method is a numerical technique with high accuracy, exponential rates of convergence and easy to use in finite and infinite domains for different problems ([23]-[25]).

The ordinary and partial fractional differential equations have been the focus of many studies due to their frequent appearance in various applications in fluid mechanics, visco-elasticity, biology, physics and engineering. Consequently, considerable attention has been given to the solutions of ODEs of physical interest ([26]-[28]). The non-linear ODEs which governing the physical problem were solved numerically using the SCM based on Chebyshev approximations of the third kind.

Nevertheless, the motivation behind this present work is to study the numerical solution by using the spectral collocation method based on Chebyshev polynomials of the third-kind for the Casson fluid flow over an unsteady stretching sheet with internal heat generation, viscous dissipation and variable heat flux involving boundary conditions of slip effect.

2. Formulation of the problem

In this section, we consider the unsteady two-dimensional laminar flow and heat transfer of a non-Newtonian Casson flow over an unsteady stretching sheet in the presence of heat generation, viscous dissipation and variable heat flux. Also, we assume that the $x-$ axis is chosen along the plane of the sheet and the $y-$ axis is taken normal to the plane. We suppose that the surface

starts stretching from rest with the velocity $U(x,t)$ which can be defined as:

$$U = \frac{cx}{1-\alpha t}, \tag{1}$$

where α and c are positive constants with dimension reciprocal time and t is the time. Here, c is the initial stretching rate. Also, we must observe that the adopted formulation of the sheet velocity in Eq. (1) is valid only for times $t < \alpha^{-1}$ unless $\alpha = 0$. Likewise, the surface heat flux $q_s(x,t)$ at the stretching sheet is assumed to vary with the power of distance x from the slit and with the power of time factor as [12]:

$$q_s(x,t) = -\kappa \frac{\partial T}{\partial y} = T_0 \frac{dx^r}{(1-\alpha t)^{m+\frac{1}{2}}}, \tag{2}$$

where κ is the fluid thermal conductivity, T is the temperature of the fluid, T_0 is the reference temperature, d is constant, r and m are space and time indices, respectively. The rheological equation of state for an isotropic and incompressible flow of a Casson fluid is [20]-[21]:

$$\tau_{ij} = \begin{cases} 2(\mu_B + P_y/\sqrt{2\pi})e_{ij}, & \pi > \pi_c \\ 2(\mu_B + P_y/\sqrt{2\pi_c})e_{ij}, & \pi < \pi_c \end{cases}$$

Here, τ_{ij} is the $(i,j)-th$ component of the stress tensor, $\pi = e_{ij}e_{ij}$ and e_{ij} is the $(i,j)-th$ component of the deformation rate, π is the product of the deformation rate with itself, π_c is a critical value of this product based on the non-Newtonian model, μ_B is the plastic dynamic viscosity of the non-Newtonian fluid and P_y is the yield stress of the fluid. So, for shear stress less than the yield stress P_y the fluid exhibits no motion i.e., it behaves like a solid, but when the shear stress greater than P_y it shows its flow characters. Likewise, the heat generation/absorbation term Q can be assumed as follows [22]:

$$Q = \begin{cases} Q_0(T - T_\infty), & T \geq T_\infty \\ 0, & T < T_\infty \end{cases}, \tag{3}$$

where Q_0 is the heat generation/absorption coefficient.

The governing time-dependent velocity and temperature fields obey such type of flow are given by :

$$\frac{\partial u}{\partial x} + \frac{\partial v}{\partial y} = 0, \tag{4}$$

$$\frac{\partial u}{\partial t} + u\frac{\partial u}{\partial x} + v\frac{\partial u}{\partial y} = \nu(1+\frac{1}{\beta})\frac{\partial^2 u}{\partial y^2} - \frac{\sigma B_0^2}{\rho}u, \tag{5}$$

$$\frac{\partial T}{\partial t} + u\frac{\partial T}{\partial x} + v\frac{\partial T}{\partial y} = \frac{\kappa}{\rho c_p}\frac{\partial^2 T}{\partial y^2} + \frac{\nu}{c_p}(1+\frac{1}{\beta})\left(\frac{\partial u}{\partial y}\right)^2 + \frac{Q_0}{\rho c_p}(T - T_\infty), \tag{6}$$

where u and v are the velocity components along the x and y directions, respectively. ρ is the fluid density, $\beta = \mu_B\sqrt{2\pi_c}/P_y$ is the Casson parameter and c_p is the specific heat at constant pressure.

The appropriate boundary conditions for the present problem are :

$$u = U(x,t) + N_1\left(1+\frac{1}{\beta}\right)\frac{\partial u}{\partial y}, \qquad v = 0, \qquad -\kappa\frac{\partial T}{\partial y} = q_s(x,t) \qquad at \qquad y = 0, \tag{7}$$

$$u \to 0, \qquad T \to T_\infty, \qquad as \qquad y \to \infty. \tag{8}$$

Here $N_1 = N(1-\alpha t)^{\frac{1}{2}}$ is the velocity slip factor which changes with time, N is the initial value of velocity factor. The mathematical analysis of the problem is simplified by introducing the following dimensionless coordinates:

$$\eta = (\frac{c}{\nu})^{\frac{1}{2}}(1-\alpha t)^{\frac{-1}{2}}y, \qquad u = \frac{cx}{1-\alpha t}f'(\eta), \qquad v = -\frac{\sqrt{c\nu}}{(1-\alpha t)^{\frac{1}{2}}}f(\eta), \tag{9}$$

$$T = T_\infty + T_0(\frac{dx^r}{\kappa\sqrt{c/\nu}})(1-\alpha t)^{-m}\theta(\eta). \tag{10}$$

Eqs.(9)-(10) are valid only for $\alpha t \ll 1$, where $f(\eta)$ is the dimensionless stream function and $\theta(\eta)$ is the dimensionless temperature.

Using Eqs. (9)-(10), the mathematical problem defined in Eqs. (5)-(8) are then transformed into a set of ordinary differential equations and their associated boundary conditions :

$$\left(1+\frac{1}{\beta}\right)f''' + ff'' - f'^2 - S(\frac{\eta}{2}f'' + f') - Mf' = 0, \tag{11}$$

$$\frac{1}{Pr}\theta'' + f\theta' - rf'\theta - S(\frac{\eta}{2}\theta' + m\theta) + Ec\left(1+\frac{1}{\beta}\right)f''^2 + \gamma\theta = 0, \tag{12}$$

$$f = 0, \qquad f' = 1, \qquad \theta' = -1 \qquad at \qquad \eta = 0 \tag{13}$$

$$f' \to 0, \quad \theta \to 0 \qquad as \qquad \eta \to \infty \tag{14}$$

where a prime denotes differentiation with respect to η, $S = \frac{\alpha}{c}$ is the unsteadiness parameter, $Ec = \frac{U^2}{c_p\Delta T}$ is the local Eckert number, $\Delta T = T_0(\frac{dx^r}{\kappa\sqrt{c/\nu}})(1-\alpha t)^{-m}$, $\gamma = \frac{xQ_0}{U\rho c_p}$ is the local heat generation (> 0) or absorption (< 0) parameter and $Pr = \frac{\rho\nu c_p}{\kappa}$ is the Prandtl number.

In engineering and practical applications, our interest lies in the investigation of the important physical quantities of the flow behavior and heat transfer characteristics by analyzing the non-dimensional local skin-friction coefficient (Cf_x) or the fractional drag coefficient and the local Nusselt number (Nu_x). These non-dimensional parameters are defined as follows :

$$Cf_x = -2Re_x^{\frac{-1}{2}}\left(1+\frac{1}{\beta}\right)f''(0), \quad Nu_x = \frac{Re_x^{\frac{1}{2}}}{\theta(0)}, \tag{15}$$

where $Re_x = \frac{Ux}{\nu}$ is the local Reynolds number.

3. Procedure of solution

3.1. Approximate the solution

The third-type of Chebyshev polynomials of degree n can be defined as follows [29]:

$$V_n(y) = \frac{\cos((n+0.5)\theta)}{\cos(0.5\theta)}, \qquad y = \cos(\theta), \qquad 0 \le \theta \le \pi.$$

These functions can be determined by using the following recurrence form [30]:

$$V_{n+1}(y) = 2yV_n(y) - V_{n-1}(y), \quad V_0(y) = 1, \quad V_1(y) = 2y - 1, \quad n = 1, 2, \ldots .$$

In this paper, we will use these functions on $[0, \hbar]$, so we can construct the so-called shifted Chebyshev polynomials by using the linear transform $y = (2/\hbar)\eta - 1$. This type of functions will be denoted and defined as $\overline{\overline{\mathbb{C}}}_n(\eta) = V_n((2/\hbar)\eta - 1)$, where $\overline{\overline{\mathbb{C}}}_0(\eta) = 1$, $\overline{\overline{\mathbb{C}}}_1(\eta) = (4/\hbar)\eta - 3$. The most common and useful formula of $\overline{\overline{\mathbb{C}}}_n(\eta)$ takes the following analytic form [31]:

$$\overline{\overline{\mathbb{C}}}_n(\eta) = \sum_{k=0}^{n} (-1)^k 2^{2n-2k} \, \frac{(2n+1)\Gamma(2n-k+1)}{\hbar^{n-k}\,\Gamma(k+1)\,\Gamma(2n-2k+2)} \, \eta^{n-k}, \qquad n = 2, 3, \ldots . \tag{16}$$

It is easy to find that $\overline{\overline{\mathbb{C}}}_k(0) = (-1)^k(2k+1)$, $\overline{\overline{\mathbb{C}}}_k(1) = 1$, $k = 0, 1, 2 \ldots$. The function $\psi(\eta) \in L_2[0, 1]$ may be defined as an infinite series sum as follows:

$$\psi(\eta) = \sum_{\ell=0}^{\infty} \sigma_\ell \, \overline{\overline{\mathbb{C}}}_\ell(\eta), \qquad \sigma_\ell = \frac{2}{\pi} \int_0^1 \sqrt{\frac{\eta}{1-\eta}} \psi(\eta) \, \overline{\overline{\mathbb{C}}}_\ell(\eta) \, d\eta, \qquad \ell = 0, 1, \ldots . \tag{17}$$

We take the first $(m+1)$-terms of (17) to obtain the following approximation form

$$\psi_m(\eta) = \sum_{\ell=0}^{m} \sigma_\ell \, \overline{\overline{\mathbb{C}}}_\ell(\eta). \tag{18}$$

Remarks concerning the convergence:

1. In [31], Khader found and proved that the series (18) of the shifted Chebyshev expansion is uniformly convergent if the function $\psi(\eta)$ satisfies the conditions; $\psi''(\eta) \in L_2[0, 1]$; and $|\psi''(\eta)| \le \kappa$; for some constant κ, and in this case he derived that $|\sigma_\ell| < \kappa/\ell^2$, $\ell = 1, 2, \ldots$.

2. He derived a formula for the upper bound of the error $\|E_m\| = \|\psi - \psi_m\|$ in approximating the function $\psi(\eta)$ by $\psi_m(\eta)$ in the case that the function $\psi(\eta) \in C^m[0, 1]$, i,e.

$$\|E_m\| \le \frac{\Lambda \Delta^{m+1}}{(m+1)!} \sqrt{\frac{\pi}{2}},$$

where $\Lambda = \max_{\eta \in [0,1]} \psi^{(m+1)}(\eta)$, and $\Delta = \max[\eta_0, \eta - \eta_0]$.

Also in this subsection, we can use the formula (16) and some properties of the differential operator to give an approximate formula of $D^{(n)}\psi_m(\eta)$ directly through the following theorem.

Theorem 1. *([31], [32])*

Suppose that we approximate the function $\psi(\eta)$ in the form (18) then $D^{(n)}(\psi_m(\eta))$ can be defined as:

$$D^{(n)}(\psi_m(\eta)) = \sum_{\ell=n}^{m} \sum_{k=0}^{\ell-n} \sigma_\ell \, \Upsilon_{\ell,k,n} \, \eta^{\ell-k-n}, \quad \Upsilon_{\ell,k,\nu} = \frac{(-1)^k 2^{2\ell-2k}(2n+1)\,(2\ell-k)!(\ell-k)!}{\hbar^{n-k}(k!)\,\Gamma(2\ell-2k+2)\,\Gamma(\ell-k+1-n)}. \tag{19}$$

3.2. Procedure solution using SCM

We will implement the SCM to solve the system (**??**)-(**??**) numerically. We approximate $f(\eta)$, and $\theta(\eta)$ by $f_N(\eta)$, and $\theta_N(\eta)$, respectively as follows:

$$f_N(\eta) = \sum_{\ell=0}^{N} a_\ell \, \tilde{\tilde{\mathbb{C}}}_\ell(\eta), \qquad \theta_N(\eta) = \sum_{\ell=0}^{N} b_\ell \, \tilde{\tilde{\mathbb{C}}}_\ell(\eta). \tag{20}$$

By using Eqs.(**??**)-(**??**), (20) and the formula (19), we can obtain:

$$\begin{aligned} &\left(1+\frac{1}{\beta}\right) \sum_{\ell=3}^{N} \sum_{k=0}^{\ell-3} a_\ell \, \Upsilon_{\ell,k,3} \, \eta^{\ell-k-3} + \left(\sum_{\ell=0}^{N} a_\ell \, \tilde{\tilde{\mathbb{C}}}_\ell(\eta)\right) \left(\sum_{\ell=2}^{N} \sum_{k=0}^{\ell-2} a_\ell \, \Upsilon_{\ell,k,2} \, \eta^{\ell-k-2}\right) \\ &\quad - \left(\sum_{\ell=1}^{N} \sum_{k=0}^{\ell-1} a_\ell \, \Upsilon_{\ell,k,1} \, \eta^{\ell-k-1}\right)^2 - \frac{\eta}{2} S \left(\sum_{\ell=2}^{N} \sum_{k=0}^{\ell-2} a_\ell \, \Upsilon_{\ell,k,2} \, \eta^{\ell-k-2}\right) \\ &\quad - (S+M) \left(\sum_{\ell=1}^{N} \sum_{k=0}^{\ell-1} a_\ell \, \Upsilon_{\ell,k,1} \, \eta^{\ell-k-1}\right) = 0, \end{aligned} \tag{21}$$

$$\begin{aligned} &\left(\frac{1}{Pr}\right) \left(\sum_{\ell=2}^{N} \sum_{k=0}^{\ell-2} b_\ell \, \Upsilon_{\ell,k,2} \, \eta^{\ell-k-2}\right) + \left(\sum_{\ell=0}^{N} a_\ell \, \tilde{\tilde{\mathbb{C}}}_\ell(\eta)\right) \left(\sum_{\ell=1}^{N} \sum_{k=0}^{\ell-1} b_\ell \, \Upsilon_{\ell,k,1} \, \eta^{\ell-k-1}\right) - r \left(\sum_{\ell=0}^{N} b_\ell \, \tilde{\tilde{\mathbb{C}}}_\ell(\eta)\right) \cdot \\ &\left(\sum_{\ell=1}^{N} \sum_{k=0}^{\ell-1} a_\ell \, \Upsilon_{\ell,k,1} \, \eta^{\ell-k-1}\right) - S \left(0.5\eta \sum_{\ell=1}^{N} \sum_{k=0}^{\ell-1} b_\ell \, \Upsilon_{\ell,k,1} \, \eta^{\ell-k-1} + m \sum_{\ell=0}^{N} b_\ell \, \tilde{\tilde{\mathbb{C}}}_\ell(\eta)\right) \\ &+ Ec \left(1+\frac{1}{\beta}\right) \left(\sum_{\ell=2}^{N} \sum_{k=0}^{\ell-2} a_\ell \, \Upsilon_{\ell,k,2} \, \eta^{\ell-k-2}\right)^2 + \gamma \left(\sum_{\ell=0}^{N} b_\ell \, \tilde{\tilde{\mathbb{C}}}_\ell(\eta)\right) = 0. \end{aligned} \tag{22}$$

The previous equations (21)-(22) will be collocated at N of nodes η_p as follows:

$$\left(1+\frac{1}{\beta}\right)\sum_{\ell=3}^{N}\sum_{k=0}^{\ell-3} a_\ell\,\Upsilon_{\ell,k,3}\,\eta_p^{\ell-k-3}+\left(\sum_{\ell=0}^{N} a_\ell\,\bar{\bar{\mathbb{C}}}_\ell(\eta_p)\right)\left(\sum_{\ell=2}^{N}\sum_{k=0}^{\ell-2} a_\ell\,\Upsilon_{\ell,k,2}\,\eta_p^{\ell-k-2}\right)$$
$$-\left(\sum_{\ell=1}^{N}\sum_{k=0}^{\ell-1} a_\ell\,\Upsilon_{\ell,k,1}\,\eta_p^{\ell-k-1}\right)^2-\frac{\eta_p}{2}\,S\left(\sum_{\ell=2}^{N}\sum_{k=0}^{\ell-2} a_\ell\,\Upsilon_{\ell,k,2}\,\eta_p^{\ell-k-2}\right) \tag{23}$$
$$-(S+M)\left(\sum_{\ell=1}^{N}\sum_{k=0}^{\ell-1} a_\ell\,\Upsilon_{\ell,k,1}\,\eta_p^{\ell-k-1}\right)=0,$$

$$\left(\frac{1}{Pr}\right)\left(\sum_{\ell=2}^{N}\sum_{k=0}^{\ell-2} b_\ell\,\Upsilon_{\ell,k,2}\,\eta_p^{\ell-k-2}\right)+\left(\sum_{\ell=0}^{N} a_\ell\,\bar{\bar{\mathbb{C}}}_\ell(\eta_p)\right)\left(\sum_{\ell=1}^{N}\sum_{k=0}^{\ell-1} b_\ell\,\Upsilon_{\ell,k,1}\,\eta_p^{\ell-k-1}\right)$$
$$-r\left(\sum_{\ell=0}^{N} b_\ell\,\bar{\bar{\mathbb{C}}}_\ell(\eta_p)\right)\left(\sum_{\ell=1}^{N}\sum_{k=0}^{\ell-1} a_\ell\,\Upsilon_{\ell,k,1}\,\eta_p^{\ell-k-1}\right)-S\left(0.5\eta_p\sum_{\ell=1}^{N}\sum_{k=0}^{\ell-1} b_\ell\,\Upsilon_{\ell,k,1}\,\eta_p^{\ell-k-1}+m\sum_{\ell=0}^{N} b_\ell\,\bar{\bar{\mathbb{C}}}_\ell(\eta_p)\right)$$
$$+Ec\left(1+\frac{1}{\beta}\right)\left(\sum_{\ell=2}^{N}\sum_{k=0}^{\ell-2} a_\ell\,\Upsilon_{\ell,k,2}\,\eta_p^{\ell-k-2}\right)^2+\gamma\left(\sum_{\ell=0}^{N} b_\ell\,\bar{\bar{\mathbb{C}}}_\ell(\eta_p)\right)=0. \tag{24}$$

In addition, the boundary conditions (**??**)-(**??**) can be expressed by substituting from Eq.(20) in (**??**)-(**??**) to find the following equations:

$$\sum_{\ell=0}^{N}(-1)^\ell(2\ell+1)\,a_\ell=0,\qquad \sum_{\ell=0}^{N} a_\ell\,\bar{\bar{\mathbb{C}}}'_\ell(0)=1,\qquad \sum_{\ell=0}^{N} a_\ell\,\bar{\bar{\mathbb{C}}}'_\ell(\hbar)=0, \tag{25}$$

$$\sum_{\ell=0}^{N} b_\ell\,\bar{\bar{\mathbb{C}}}'_\ell(0)=-1,\qquad \sum_{\ell=0}^{N} b_\ell=0. \tag{26}$$

Eqs.(23)-(24), together with equations (25)-(26), give a system of $2(N+1)$ algebraic equations. This system will solve for the unknowns a_ℓ, b_ℓ, $\ell=0,1,...,N$, by using the Newton iteration method (NIM).

4. Results and discussion

The previous analysis discussed the effect of variable heat flux on MHD non-Newtonian slip casson fluid flow and heat transfer over an unsteady stretching sheet in the presence of viscous dissipation and internal heat generation or absorption. Now in this section, we will discuss the behavior of the physical parameters governing the proposed model, namely, magnetic parameter M, the Casson parameter β, unsteady parameter S, time indices parameter m, space indices parameter r, the local heat generation or absorption parameter γ, the velocity slip parameter λ, the Prandtl number Pr and the local Eckert number Ec. Figures 1 (a) and 1 (b) examine the

influence of magnetic number M on the velocity and temperature profiles respectively. Figure 1 (a) exhibits that the velocity is a decreasing function of M, whereas Figure 1 (b) is an increasing function of the same parameter M.

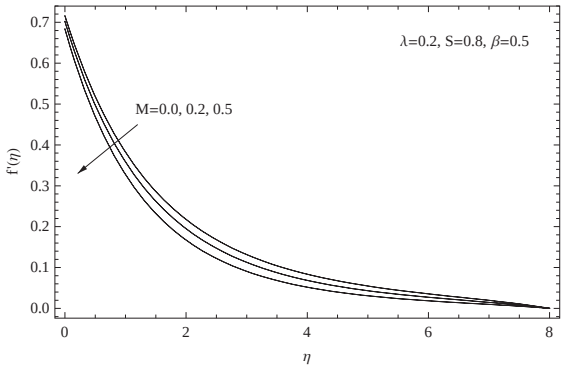

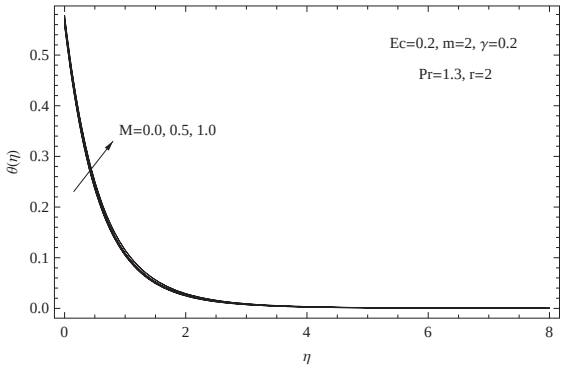

Figure 1. (a) Velocity distribution for M (b) Temperature distribution for M

Fig. 2 (a). is plotted to discuss the dimensionless velocity distribution inside the boundary layer for different values of unsteadiness parameter S. From this figure it can be noted that an increase in the unsteadiness parameter leads to a fall in the flow velocity distribution inside the boundary layer. On the other hand, due to the presence of heat flux along the sheet, it is found that the temperature distribution along the boundary layer and the wall temperature $\theta(0)$ decreases with an increase in the same parameter as we can see from Fig. 2 (b). This shows the important fact that the rate of cooling is much faster for higher values of the unsteadiness parameter whereas it may take a longer cooling time for smaller values of the unsteadiness parameter.

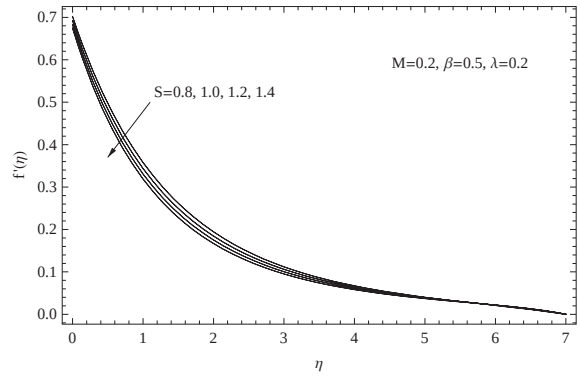

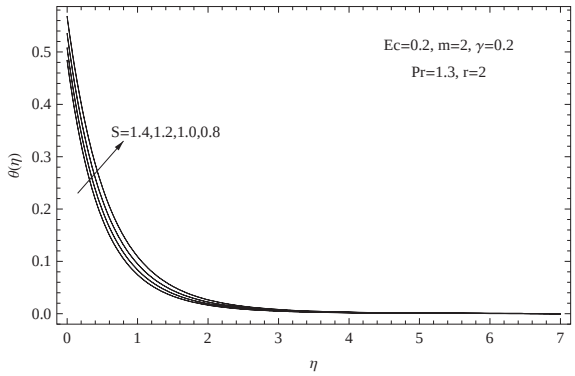

Figure 2. (a) Velocity distribution for S (b) Temperature distribution for S

We next show in Fig. 3 (a), the velocity distribution against the similarity variable η for various values of Casson parameter β. From this figure it can be seen that increasing the Casson parameter leads to increases in velocity distribution along the sheet but the reverse is true away from the sheet. In addition, the thickness of the boundary layer is found to decreases with increasing the Casson parameter. The temperature profiles for different values of the same

parameter is presented in Fig. 3 (b). This figure reveals that both the temperature in the thermal boundary layer and the wall temperature $\theta(0)$ increases for increasing the Casson parameter but in weakly differences between values of the Casson parameter.

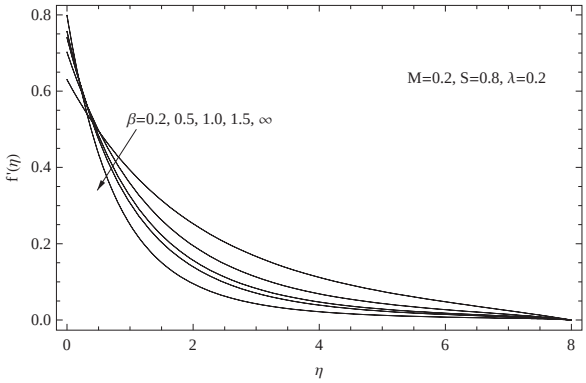

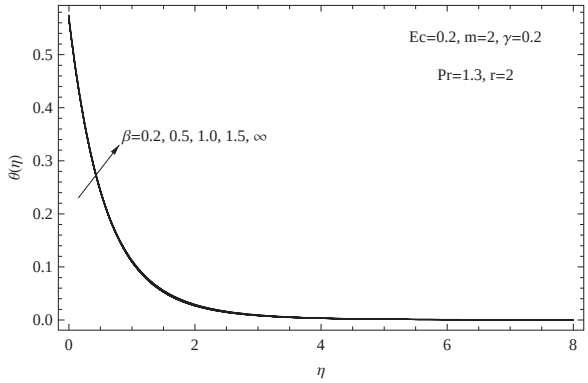

Figure 3. (a) Velocity distribution for β (b) Temperature distribution for β

Figs. 4 (a) and 4 (b) have been drawn, to elucidate the influence of the velocity slip parameter λ on the velocity and temperature profiles. From figure 4 (a), it is observed that both the velocity distribution inside the boundary layer and the boundary layer thickness are decreased as the slip velocity parameter increases. Physically, with slip condition, the slipping fluid decrease the surface skin-friction values between the fluid and the stretching sheet. So, increasing the value of the slip velocity parameter will decrease the flow velocity in the region of the boundary layer. The dimensionless temperature distribution within the boundary layer region for the slip velocity parameter is illustrated in Fig. 4 (b). From this figure we can noted that an increase in the velocity slip parameter may result in an augmentation for both the temperature of the wall $\theta(0)$ and the fluid temperature distribution in the thermal boundary layer.

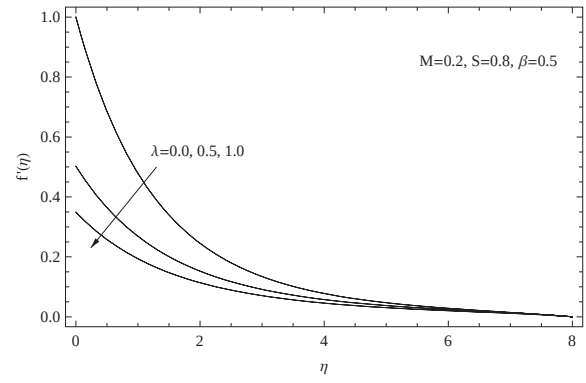

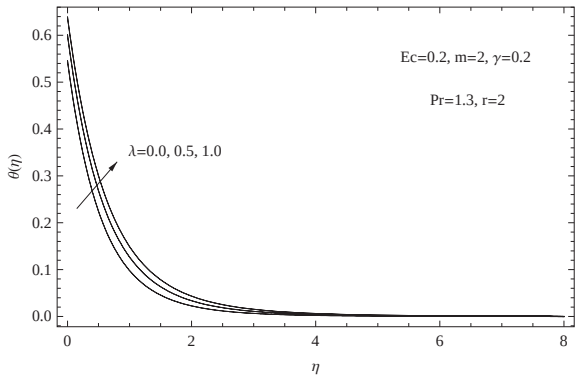

Figure 4. (a) Velocity distribution for λ (b) Temperature distribution for λ

Figure 5 (a), shows the effect of the Prandtl number Pr on the temperature profiles above the sheet. From this figure, it is noticed that, a decrease in the Prandtl number may result in an enhancement on thermal boundary layer thickness, temperature distribution and the temperature

of the wall $\theta(0)$. This phenomenon is observed because the higher values of Prandtl number correspond to the weaker thermal diffusivity. The effect of Eckert number on the temperature profile, is shown in Fig. 5 (b). It is evident that the effect of increasing Eckert number is to increase both the temperature distribution along the boundary layer and the temperature of the surface $\theta(0)$. This is of course a consequence of the fact that for higher values of the Eckert number, there is significant generation of heat due to viscous dissipation near the sheet. So, viscous dissipation in a flow due to stretching sheet is beneficial for gaining temperature.

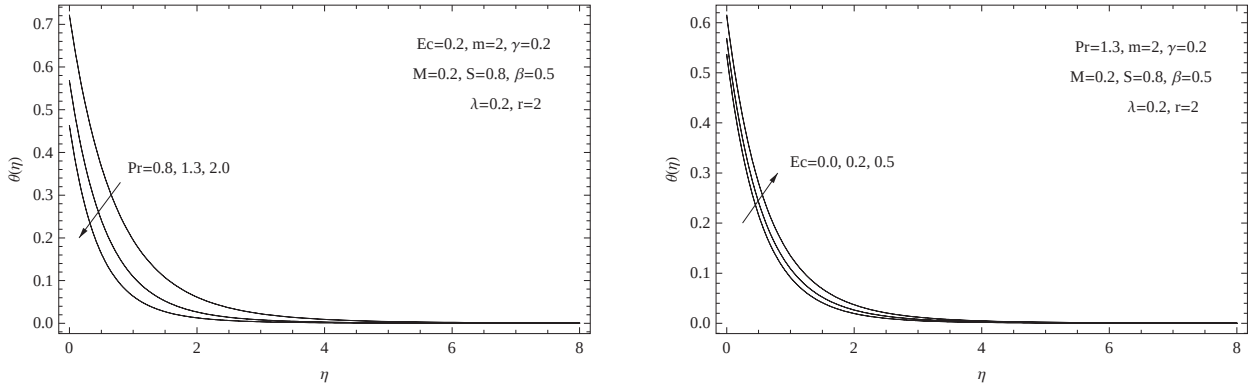

Figure 5. (a) Temperature distribution for Pr (b) Temperature distribution for Ec

Figs. 6 (a) and 6 (b) illustrate that how profiles of temperature distribution are affected by the variations in the space index parameter r or (the time index parameter m) when other parameters remain fixed. These figures indicate that the dimensionless temperature profile turns depressed for increasing value of two parameters. Likewise, it is observed that the effect of increasing these two parameters will cause a drop in the temperature of the wall $\theta(0)$.

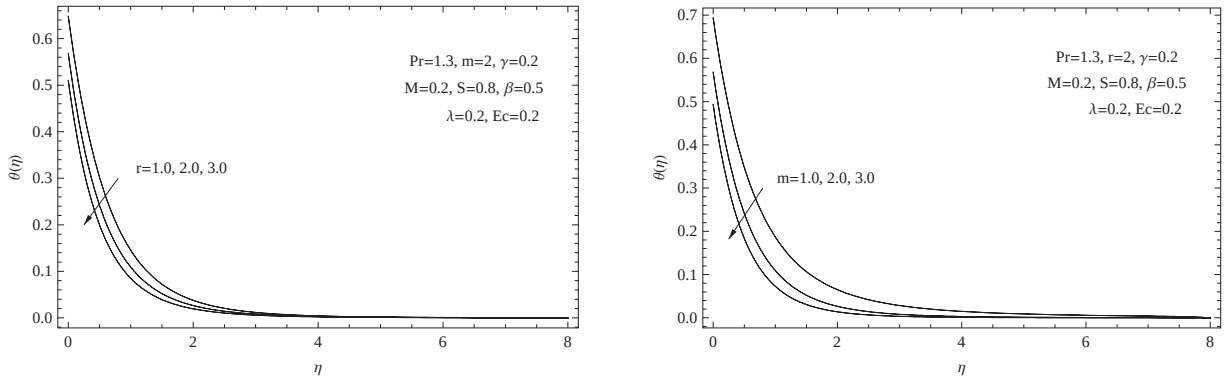

Figure 6. (a) Temperature distribution for r (b) Temperature distribution for m

Last, but not least, Fig. 7 illustrate that how profiles of temperature distribution are affected by the variations in the heat generation/absorption parameter γ when other parameters remain fixed. This figure indicate that the thermal boundary-layer thicknesses increase when the internal heat generation parameters $\gamma > 0$ becomes stronger whereas the internal heat absorption

parameters $\gamma < 0$ have the opposite effect. Also, it is noticed that the highest temperature distribution for the fluid in the boundary layer was obtained with the greatest heat generation parameters $\gamma > 0$. Likewise, it is shown that the effect of heat absorption parameters $\gamma < 0$ causes a drop in the temperature distribution as the heat following from the sheet is absorbed.

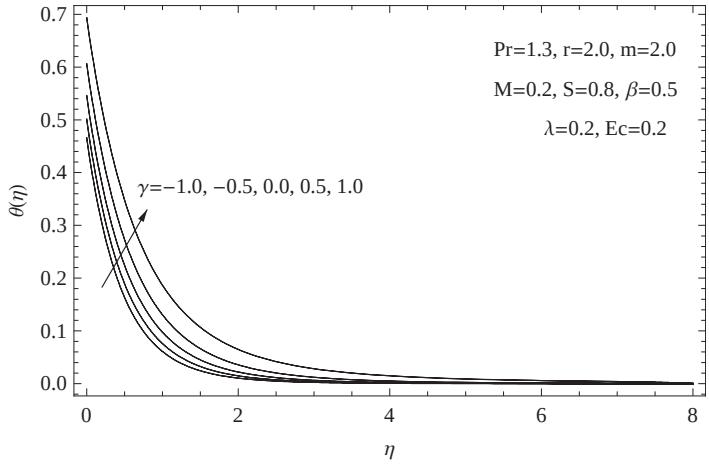

Figure 7. Temperature distribution for γ

Table 1 reveal the effect of different values of physical governing parameters of the magnetic parmaeter M, the Casson parameter β, unsteady parameter S, time indices parameter m, space indices parameter r, the heat generation parameter, the Prandtl number Pr, the velocity slip parameter λ and the Eckert number Ec as these are required for the evaluation of the local skin-friction coefficient $\frac{1}{2}Cf_xRe_x^{\frac{1}{2}}$ and the local Nusselt number $Nu_xRe_x^{\frac{-1}{2}}$. It is seen that the increase in unsteady parameter causes increase in both the skin-friction coefficient and local Nusselt number. Also, the local skin-friction coefficient decreases by increasing the Casson parameter, whereas the local Nusselt number increases with the increasing values of it. With the increase in the slip velocity parameter λ both the local skin-friction coefficient and the local Nusselt number are decreases. Moreover, it is noticed that increases in the values of the Eckert number and the heat generation parameter leads to a decrease in the local Nusselt number. On the other hand, an increase in the Prandtl number causes an increase in the local Nusselt number. This is because fluid with a higher value of Prandtl number posses a large heat capacity, and hence intensifies the heat transfer. Finally, the local Nusselt number increases as the space indices parameter, the heat absorption parameter and time indices parameter increases.

Table 1. Variation of $-(1+\frac{1}{\beta})f''(0)$ and $\frac{1}{\theta(0)}$ for various values of $M, S, \beta, \lambda, \gamma, Ec, r, m$ and Pr.

M	S	β	λ	Pr	Ec	r	m	γ	$-(1+\frac{1}{\beta})f''(0)$	$\frac{1}{\theta(0)}$
0.0	0.8	0.5	0.2	1.3	0.2	2.0	2.0	0.2	1.42101	1.78389
0.2	0.8	0.5	0.2	1.3	0.2	2.0	2.0	0.2	1.48953	1.76116
0.5	0.8	0.5	0.2	1.3	0.2	2.0	2.0	0.2	1.58118	1.73096
0.2	0.8	0.5	0.2	1.3	0.2	2.0	2.0	0.2	1.48975	1.76104
0.2	1.0	0.5	0.2	1.3	0.2	2.0	2.0	0.2	1.53819	1.86843
0.2	1.0	0.5	0.2	1.3	0.2	2.0	2.0	0.2	1.58376	1.97008
0.2	1.4	0.5	0.2	1.3	0.2	2.0	2.0	0.2	1.62672	2.06688
0.2	0.8	0.2	0.2	1.3	0.2	2.0	2.0	0.2	1.84905	1.74277
0.2	0.8	0.5	0.2	1.3	0.2	2.0	2.0	0.2	1.48953	1.76116
0.2	0.8	1.0	0.2	1.3	0.2	2.0	2.0	0.2	1.29823	1.76601
0.2	0.8	1.5	0.2	1.3	0.2	2.0	2.0	0.2	1.21724	1.76669
0.2	0.8	0.5	0.0	1.3	0.2	2.0	2.0	0.2	2.31847	1.83242
0.2	0.8	0.5	0.5	1.3	0.2	2.0	2.0	0.2	0.99485	1.66516
0.2	0.8	0.5	1.0	1.3	0.2	2.0	2.0	0.2	0.650784	1.56523
0.2	0.8	0.5	0.2	0.8	0.2	2.0	2.0	0.2	1.48953	1.38704
0.2	0.8	0.5	0.2	1.3	0.2	2.0	2.0	0.2	1.48953	1.76116
0.2	0.8	0.5	0.2	2.0	0.2	2.0	2.0	0.2	1.48953	2.16256
0.2	0.8	0.5	0.2	1.3	0.0	2.0	2.0	0.2	1.48953	1.86381
0.2	0.8	0.5	0.2	1.3	0.2	2.0	2.0	0.2	1.48953	1.76116
0.2	0.8	0.5	0.2	1.3	0.5	2.0	2.0	0.2	1.48953	1.62677
0.2	0.8	0.5	0.2	1.3	0.2	1.0	2.0	0.2	1.48953	1.54332
0.2	0.8	0.5	0.2	1.3	0.2	2.0	2.0	0.2	1.48953	1.76116
0.2	0.8	0.5	0.2	1.3	0.2	3.0	2.0	0.2	1.48953	1.96055
0.2	0.8	0.5	0.2	1.3	0.2	2.0	1.0	0.2	1.48953	1.44167
0.2	0.8	0.5	0.2	1.3	0.2	2.0	2.0	0.2	1.48953	1.76116
0.2	0.8	0.5	0.2	1.3	0.2	2.0	1.0	0.2	1.48953	2.02621
0.2	0.8	0.5	0.2	1.3	0.2	2.0	2.0	-1.0	1.48953	2.14588
0.2	0.8	0.5	0.2	1.3	0.2	2.0	2.0	-0.5	1.48953	1.99512
0.2	0.8	0.5	0.2	1.3	0.2	2.0	2.0	0.0	1.48953	1.83129
0.2	0.8	0.5	0.2	1.3	0.2	2.0	2.0	0.5	1.48953	1.64976
0.2	0.8	0.5	0.2	1.3	0.2	2.0	2.0	1.0	1.48953	1.44167

5. Conclusions

The boundary layer flow and heat transfer of a Casson fluid over an unsteady stretching sheet with slip effects, viscous dissipation, variable heat flux and internal heat generation/absorption is analyzed here. The governing partial differential equations were converted into ordinary differential equations by using a suitable dimensionless transformation, which are solved numerically by employing the spectral collocation method based on Chebyshev polynomials of the third-kind. It was found that the effect of increasing values of the unsteadiness parameter, heat absorption parameter or the Prandtl number is to enhance the local Nusselt number. Also, it was obtained the local skin-friction coefficient and the local Nusselt number are decreases as the slip velocity parameter increases. On the other hand, it was obtained that the local Nusselt number decreases as both the heat generation parameter or the Eckert number increases but the reverse is true for the Casson parameter. Moreover, it is interesting to find that as the time indices parameter or the space indices parameter increases in magnitude, causes the local Nusselt number to increase.

Acknowledgements

The author thanks the Deanship of Academic Research, Imam Mohammad Ibn Saud Islamic University (IMSIU), Riyadh, KSA, for the financial support of the project number (41xxxx).

References

[1] Crane, L. J. Flow past a stretching plate. Zeitschrift für angewandte Mathematik und Physik, 21, (1970) 645-647.

[2] Gupta, P. S. and Gupta, A. S., Heat and mass transfer on a stretching sheet with suction or blowing. Can. J. Chem. Eng, 55 (1977) 744-746.

[3] Grubka, L. J. and Bobba, K. M. Heat transfer characteristics of a continuous stretching surface with variable temperature. ASME J. Heat Transfer 107 (1985) 248-250.

[4] Chen, C. K., Char, M., Heat transfer on a continuous, stretching surface with suction or blowing. J. Math. Anal. Appl. 35 (1988)568-580.

[5] Ali, M. E., Heat transfer characteristics of a continuous stretching surface. Warme Stoffubertrag 29 (1994) 227-234.

[6] Pop, I. and Na, T., Unsteady flow past a stretching sheet. Mechanics Research Communications. 23 (1996) 413-422.

[7] Elbashbeshy E. M. A., Bazid M. A. A., Heat transfer over an unsteady stretching surface. Heat and Mass Transfer 41 (2004) 1-4.

[8] Mukhopadyay, S., Effect of thermal radiation on unsteady mixed convection flow and heat transfer over a porous stretching surface in porous medium. International Journal of Heat and Mass Transfer 52 (2009) 3261-3265.

[9] Ishak,A., Nazar, R. and Pop, I., Heat Transfer over an Unsteady Stretching Permeable Surface with Prescribed Wall Temperature. Non-linear Analysis: Real World Applications 10 (2009) 2909-2913.

[10] Elbashbeshy, E. M.A. and Aldawody, D.A., Effects of thermal radiation and magnetic field on unsteady mixed convection flow and heat transfer over a porous stretching surface. International Journal of Nonlinear Science 9 (2010) 448-454.

[11] Ching-Yang Cheng, Soret and Dufour effects on natural convection boundary layer flow over a vertical cone in a porous medium with constant wall heat and mass fluxes. International Communications in Heat and Mass Transfer 38 (2011) 44-48.

[12] Megahed, A. M., Variable heat flux effect on MHD flow and heat transfer over an unsteady stretching sheet in the presence of thermal radiation. Canadian Journal of Physics 92 (2014) 86-91.

[13] Bhattacharyya, K., Hayat, T. and Alsaedi, A., Exact solution for boundary layer flow of Casson fluid over a permeable stretching/shrinking sheet. ZAMM Z. Angew. Math. Mech. 94 (2014) 522-528.

[14] Mukhopadhyay, S., Ranjan De, P., Bhattacharyya, k. and Layek, G.C., Casson fluid flow over an unsteady stretching surface. Ain Shams Engineering Journal 4 (2013) 933-938.

[15] Boyd, J., Buick, J. M. and Green S., Analysis of the Casson and Carreau-Yasuda non-Newtonian blood models in steady and oscillatory flow using the lattice Boltzmann method. Phys Fluids 19 (2007) 93-103.

[16] Thompson, P. A. and Troian, S. M., A general boundary condition for liquid flow at solid surfaces. Nature, 389 (1997)360-362.

[17] Megahed, A. M., HPM for slip velocity effect on a liquid film over an unsteady stretching surface with variable heat flux. The European Physical Journal Plus 126 (2011) 1-8.

[18] Turkyilmazoglu, M. Multiple solutions of heat and mass transfer of MHD slip flow for the viscoelastic fluid over a stretching sheet. International Journal of Thermal Sciences 50 (2011) 2264-2276.

[19] Megahed, A. M. Variable viscosity and slip velocity effects on the flow and heat transfer of a power-law fluid over a non-linearly stretching surface with heat flux and thermal radiation. Rheologica Acta 51 (2012) 841-847.

[20] Shahmohamadi, H. Analytic study on non-Newtonian natural convection boundary layer flow with variable wall temperature on a horizontal plate. Meccanica, 47 (2012) 1313-1323.

[21] Mustafa, M., Hayat, T., Pop, I. and Hendi A. Stagnation-point flow and heat transfer of a Casson fluid towards a stretching sheet. Zeitschrift für Naturforschung A 67 (2012) 70-76.

[22] Mostafa A. A. Mahmoud, The effects of variable fluid properties on MHD Maxwell fluids over a stretching surface in the presence of heat generation/absorption. Chemical Engineering Communications 198 (2011) 131-146.

[23] Boyd J. P., Chebyshev and Fourier Spectral Methods, (2nd Ed. Dover), New York, USA, 2000.

[24] Khader M. M., On the numerical solutions for the fractional diffusion equation. Communications in Nonlinear Science and Numerical Simulations 16, 2535-2542 (2011).

[25] Khader M. M., Mohammed M. Babatin, Numerical treatment for solving fractional SIRC model and influenza A. Computational and Applied Mathematics 33(3), 543-556 (2014).

[26] Khader M. M., Saad K. M., A numerical study using Chebyshev collocation method for a problem of biological invasion: fractional Fisher equation. Int. J. Biomathematics, 11(8), 1-15 (2018).

[27] Khader M. M., Saad K. M., On the numerical evaluation for studying the fractional KdV, KdV-Burger's, and Burger's equations. European Physical Journal Plus 133, 1-13 (2018).

[28] Saad K. M., Khader M. M., Gomez-Aguilar J. F., and Dumitru Baleanu, Numerical solutions of the fractional Fisher's type equations with Atangana-Baleanu fractional derivative by using spectral collocation methods. Chaos 29, 1-5 (2019).

[29] Snyder M. A., Chebyshev Methods in Numerical Approximation, Prentice-Hall, Inc. Englewood Cliffs, N. J. 1966.

[30] Mason J. C., Handscomb D. C., Chebyshev Polynomials, Chapman and Hall, CRC, New York, NY, Boca Raton, 2003.

[31] Khader M. M., Saad K. M., A numerical approach for solving the problem of biological invasion (fractional Fisher equation) using Chebyshev spectral collocation method. Chaos, Solitons & Fractals, 110, 169-177 (2018).

[32] Handan C. Y., Numerical solution of fractional Riccati differential equation via shifted Chebyshev polynomials of the third kind, J. of Eng. Technology and Applied Sciences 28, 1-11 (2017).